Two distinct auto-regulatory loops operate at the *PU.1* locus in B cells and myeloid cells

*Mathias Leddin,[1] *Chiara Perrod,[1] *Maarten Hoogenkamp,[2] *Saeed Ghani,[1] Salam Assi,[3] Sven Heinz,[4] Nicola K. Wilson,[5] George Follows,[5] Jörg Schönheit,[1] Lena Vockentanz,[1] Ali M. Mosammam,[2] Wei Chen,[1] Daniel G. Tenen,[6,7] David R. Westhead,[3] Berthold Göttgens,[5] Constanze Bonifer,[2] and Frank Rosenbauer[1]

[1]Max Delbrück Center for Molecular Medicine, Berlin, Germany; [2]Leeds Institute for Molecular Medicine, University of Leeds, Leeds, United Kingdom; [3]Faculty of Biological Sciences, University of Leeds, Leeds, United Kingdom; [4]Department of Cellular and Molecular Medicine, University of California, San Diego, LA Jolla, CA; [5]Department of Haematology, Cambridge Institute for Medical Research, University of Cambridge, Cambridge, United Kingdom; [6]Harvard Stem Cell Institute, Harvard Medical School, Boston, MA; and [7]Cancer Science Institute, National University of Singapore, Republic of Singapore

The transcription factor PU.1 occupies a central role in controlling myeloid and early B-cell development, and its correct lineage-specific expression is critical for the differentiation choice of hematopoietic progenitors. However, little is known of how this tissue-specific pattern is established. We previously identified an upstream regulatory *cis* element whose targeted deletion in mice decreases PU.1 expression and causes leukemia. We show here that the upstream regulatory *cis* element alone is insufficient to confer physiologic PU.1 expression in mice but requires the cooperation with other, previously unidentified elements. Using a combination of transgenic studies, global chromatin assays, and detailed molecular analyses we present evidence that *PU.1* is regulated by a novel mechanism involving cross talk between different *cis* elements together with lineage-restricted autoregulation. In this model, PU.1 regulates its expression in B cells and macrophages by differentially associating with cell type–specific transcription factors at one of its *cis*-regulatory elements to establish differential activity patterns at other elements. (*Blood*. 2011;117(10):2827-2838)

Introduction

In the hematopoietic system, formation of the earliest myeloid and lymphoid transcriptional networks essentially depends on the transcription factor PU.1.[1] PU.1 ablation in mice leads to a fatal defect in fetal liver or newborn hematopoiesis or both, which includes the complete absence of B cells and macrophages.[2-5] The expression level of the *PU.1* gene must be tightly controlled during hematopoietic differentiation because differences in the PU.1 concentration can directly change the developmental fate of hematopoietic progenitors and can cause leukemic transformation.[6-14] Consequently, understanding how the correct PU.1 levels are established is a key step in deciphering mechanisms of hematopoietic cell diversification and tumor suppression.

We have previously identified a distal regulatory element, located at 15 kb (kilobase) and 14 kb upstream of the *PU.1* gene in the mouse, which is indispensable for proper PU.1 expression.[15] Deletion of this element (designated URE for upstream regulatory element) from the mouse genome leads to 80% decreased PU.1 expression in hematopoietic stem cells (HSCs), myeloid cells, and B cells.[13] Such URE mutants develop a multilineage differentiation block that rapidly transits into an acute myeloid leukemia.[9] However, deletion of the URE does not completely abolish *PU.1* transcription, suggesting that additional regulatory elements are driving PU.1 expression. Moreover, URE ablation affects PU.1 expression in all hematopoietic lineages, suggesting that it serves as a broad-acting regulator element but does not control lineage-specific differences in *PU.1* expression.

A number of questions have yet to be answered with respect to the regulation of *PU.1*. This includes the position and nature of the complete set of *cis*-regulatory elements, their regulatory interplay, the factors which they interact with, and in what combinations they drive the expression of this gene in different hematopoietic lineages. To address these issues, we combined transgenic rescue experiments in PU.1-knockout mice with genomewide high-resolution chromatin structure mapping in macrophages and B cells. We show that the URE alone is insufficient to confer correct regulation on the *PU.1* promoter, and we characterized myeloid-specific *PU.1 cis*-regulatory elements that are required to drive correct *PU.1* expression in mice. One of these elements is an enhancer at −12 kb, which synergizes with the URE to mediate high-level PU.1 expression. Similar to the URE, this enhancer binds PU.1. We find that CCAAT/enhancer binding protein α (C/EBPα) binds to the URE and initiates a cross talk between *cis* elements to drive myeloid-specific PU.1 expression. Our findings uncover a new molecular mechanism governing a tissue-specific cross-regulation of *cis*-regulatory element activity on the basis of auto-regulation and a differential association with cell type–specific transcription factors.

Submitted August 23, 2010; accepted December 24, 2010. Prepublished online as *Blood* First Edition paper, January 14, 2011; DOI 10.1182/blood-2010-08-302976.

The online version of this article contains a data supplement.

The publication costs of this article were defrayed in part by page charge payment. Therefore, and solely to indicate this fact, this article is hereby marked "advertisement" in accordance with 18 USC section 1734.

*M.L. C.P., M.H., and S.G share first authorship.

Methods

Mice and cell lines

PU.1$^{-/-}$, URE$^{-/-}$, and URE-TG^{+} transgenic mice containing the PU.1iresEGFP cassette have been described.[4,13,16] The transgenic Flag-PU.1 construct was generated by inserting Flag-PU.1 released from pECE-Flag-PU.1 into the *Not*I site of the pBluescript-URE/prom/β-globin transgenic plasmid described.[16] All transgenic constructs were linearized and microinjected into fertilized oocytes of FVB/N mice and implanted in uteri of pseudopregnant FVB/N mice. Founder mice were identified as described.[4,16]

416B, RAW264.7, BW5147, HL60, HM1, HPC-7, and C10 cells were cultured as described.[17-19] The URE$^{-/-}$ cell line was generated from a URE$^{-/-}$ mouse with myeloid leukemia, and the URE$^{+/+}$ control line was generated from a myeloid leukemic mouse that had received a transplant of myc-transformed donor cells. Both lines were maintained in Iscoves modified Dulbecco medium supplemented with 20% fetal calf serum and 10 ng/mL interleukin-3.

Retroviral construct and cell transduction

Plat-E cells were used for viral supernatant production as described.[9] URE$^{-/-}$ and URE$^{+/+}$ cell lines were incubated with retroviral supernatants derived from a murine stem cell virus-based tamoxifen-inducible C/EBPα-ERT-GFP construct (gift from J. Cammenga, Lund) in the presence of 8 μg/mL polybrene (hexadimethrine bromide; Sigma-Aldrich). Stably transduced cells were sorted for green fluorescent protein (GFP) expression and cultured in interleukin-3 containing Iscoves modified Dulbecco medium. C/EBPα was induced by supplementing the medium with 10μM tamoxifen (Gibco).

Genomic integrity and copy number analysis of the bacterial artificial chromosome transgenes

Copy numbers of bacterial artificial chromosome (BAC) transgenes were measured by Southern blotting with the use of *Eco*RI-digested genomic DNA and a murine 208-bp (base pair) probe located 8 kb upstream of the *PU.1* promoter. Relative signal density was calculated after exposure with a Fuji FLA-3000 PhosphorImager with the use of the TINA2.0 software. Genomic integrity of the BAC transgenes was validated by Southern blotting with the use of with *Sca*I-digested genomic DNA. Probes were generated by polymerase chain reaction (PCR) amplification with the use of the *PU.1* BAC as template. Primer pairs are available on request.

Analysis of blood

Blood samples were taken from age-matched mice (12-16 weeks) by tail puncture. Blood counts were performed with an Animal Blood Counter (Scil Animal Care Company).

Flow cytometry and cell sorting

Instruments used for flow cytometric analysis were a LSR II cytometer (BD Biosciences) and for cytometric sorting a FACSAria (BD Biosciences). Anti–mouse antibodies conjugated with fluorescein isothiocyanate, phycoerythrin (PE), PE-Cy7, PE-Cy5, allophycocyanin, allophycocyanin-Cy7, Pacific blue, or biotin were specific for the following cell surface molecules: Mac-1/CD11b (M1/70), CD3ε (145-2C11), CD4 (GK1.5), CD8α (53-6.7), B220 (RA3-6B2), Gr-1 (RB6-8C5), CD19 (1D3), immunoglobulin M (IgM; R6-60.2), Sca1 (E13-161-7), c-Kit (2B8), Fc-γRII/III (2.4G2), and CD34 (RAM34). All antibodies were from BD Biosciences, eBioscience, or Caltag Laboratories. Analysis and sorting of HSCs and myeloid progenitors were conducted as described.[20]

In vitro colony-forming assay

Colonies were analyzed with the Axio Observer.Z1 2 and the 10×/0.3 Ph1 objective. AxioVision Version 4.2 was used as software. Pictures were taken with AxioCAM Mrn. For cytospins as microscope Axioplan 2 with a 63×/1.23 oil objective and as camera AxioCam HRc was used. AxioVision Version 4.7 was used as software.

Real-time PCR

RNA was extracted according to the manufacturer's instructions with the use of Trifast (Peqlab), reverse transcribed with a cDNA synthesis kit (Fermentas), and then amplified with a 7300 Real-time PCR system (Applied Biosystems) with the use of exon-spanning primer/probe sets. All primer and probe sequences are available on request.

Design and fabrication of custom array

A series of 65 base-long oligonucleotides were designed to span the *PU.1* locus with the use of Primer3 on repeat masked sequences. Oligonucleotides were spotted in triplicate with the use of a MicroGrid II arrayer (Biorobotics/Genomic Solutions). Array design files have been submitted to ArrayExpress (accession no. A MEXP 1767).

ChIP–quantitative PCR and ChIP-chip assays

Chromatin immunoprecipitation (ChIP) assays were performed as described.[21] Antibodies used were anti-H3, anti-H3Ac9 (Upstate Biotechnology), or anti-PU.1 (Santa Cruz Biotechnology). Precipitated chromatin was analyzed by Sybr-Green Real-time PCR. Primer sequences are available on request. For ChIP-chip assays, histone 3 lysine 9 acetylation (H3K9ac) precipitated material was labeled with Cy3 and Cy5 fluorochromes, hybridized, and analyzed as described.[22]

Western blot

Western blot was conducted as described.[13] A polyclonal rabbit antibody to PU.1 (Santa Cruz Biotechnology) and a monoclonal mouse antibody to TUBULIN (Sigma) were used. The enhanced chemiluminescence system was used (Invitrogen) to detect horseradish peroxidase–coupled antibodies.

Reporter constructs and luciferase assays

All *PU.1* distal regulatory *cis* regions analyzed in this study were subcloned from BAC-clone RPCI-21 544O8 containing the mouse *PU.1* genomic sequences. Mutations in C/EBP and PU.1 binding motifs were generated as described.[16,23] Maps of all construct are available on request.

To generate cell lines stably carrying luciferase constructs, 1×10^7 RAW264.7 or Namalwa cells were electroporated with 10 μg of pXP2-based luciferase plasmids along with 1 μg of a plasmid containing a puromycin-resistance gene. Transfected cells were selected in media supplemented with 20 μg/mL puromycin (Roth) for RAW264.7 and 0.75 μg/mL for Namalwa cells. Copy numbers of integrated plasmids were determined by Southern blotting with the use of a 751-bp *Eco*RI-*Eco*RV fragment released from pXP2. Luciferase assays were conducted with the Dual-Luciferase Reporter Assay System (Promega), and all values were normalized for plasmid copy numbers.

DNaseI footprinting

DNaseI treatment of cells and naked DNA and ligation-mediated PCR were performed as described.[24] Primer sequences are available on request.

Short hairpin RNA assay

The short hairpin RNA (shRNA) sequence to knock down PU.1 expression has been described.[25] Cell lines were transfected with shRNA constructs by FuGene 6 (Roche). Forty-eight hours later 1×10^6 GFP^{+} cells were sorted, and luciferase assays were performed.

Genomewide DNaseI hypersensitivity analysis

Bone marrow–derived macrophages and splenic CD19^{+}IgM^{+} B cells were cultured as described.[26,27] DNaseI treatment was performed as described.[24] DNaseI-treated genomic DNA (10 μg) was run on an agarose gel, and

fragments in the range of 100-600 bp were cut out from a sample showing similar low-level DNaseI digestion as measured by real-time PCR analysis with the use of primers amplifying an active promoter (*Tbp* locus) or an inactive region from chromosome 2, and then purified with using a gel extraction kit (QIAGEN). For library preparation, 10 ng of DNA fragments were processed with the Illumina sample preparation kit. After library preparation, 200-bp fragments were isolated and analyzed by massively parallel DNA sequencing on an Illumina Genome Analyzer.

Datasets and genome alignment

DNaseI hypersensitivity (DHS) datasets are described in "Genomwide DNaseI hypersensitivity assay." ChIP-sequencing datasets for PU.1 and C/EBPα were from Heinz et al.[28] P300 datasets were from Ghisletti et al.[29] The raw sequence returned by the Illumina Pipeline was aligned to the mm9 assembly (NCBI Build 37) with the use of Maq.[30] All ChIP-sequencing data used in this study were remapped from raw sequence data.

Identification of DHS- and ChIP-sequencing peaks

Peak finding analysis was performed with the FindPeaks software.[31] All peaks above a threshold of minimum height were considered, corresponding to a false discovery rate of 0.1%. For the DHS data the "-trim" and "-subpeaks" flags were used to separate wide peaks at each area of enrichment, and the "triangle" fragment size distribution was used with high, low, and median fragment size values of 200, 50, and 125, respectively. A built-in control mode was performed when the method of hyperbolic sections was used. ChIP-sequencing peaks in PU.1 and C/EBPα data were identified in an identical manner with the use of FindPeaks. The high, low, and median fragment sizes were 300, 50, and 150, respectively. Overlaps between ChIP and DHS sequencing were defined by requiring the center of a peak in the ChIP dataset to lie between the upper and lower boundaries of a peak in the DHS data. The same criterion was applied to overlap DHS peaks in different cell types.

Motif analysis

De novo motif analysis was performed with the use of HOMER.[28] Motifs of length 8, 10, and 12 bp were identified on the peak sequences of length ± 100 bp from the peak center. The motif matrices generated by HOMER were scanned against TRANSFAC with the use of STAMP.[32] The top enriched known motifs with significant score were considered.

Statistical analysis

Statistical analysis was performed as described.[33]

Results

URE-driven transgenic PU.1 expression fails to rescue hematopoiesis in *PU.1*$^{-/-}$ mice

We have previously demonstrated that the URE is required for high-level PU.1 expression.[9] To test whether the URE is also sufficient to drive PU.1 expression in vivo, we used a transgenic rescue approach. We generated constructs containing the URE fused to a 2.1-kb proximal *PU.1* promoter fragment, both inserted in front of the murine PU.1 cDNA, followed by either a reporter cassette with an internal ribosomal entry site and an enhanced GFP (iresEGFP) gene or to a Flag-tag (Figure 1A). We generated 5 independent transgenic lines (2 lines containing PU.1iresEGFP and 3 lines containing Flag-PU.1), all of which expressed PU.1 or EGFP with the same pattern that we have published previously (data not shown).[16]

To test whether URE/promoter-driven PU.1 could rescue the PU.1-knockout phenotype, we bred 4 transgenic lines (2 containing Flag-PU.1 and 2 containing PU.1iresEGFP) into a *PU.1*$^{+/-}$ background. We crossed transgenic *PU.1*$^{+/-}$ (termed URE-TG^{+}*PU.1*$^{+/-}$) with nontransgenic *PU.1*$^{+/-}$ (termed URE-TG^{-}*PU.1*$^{+/-}$) animals and genotyped the offspring at weaning. From ~ 100 born pups, we did not detect any animals harboring the *PU.1*$^{-/-}$ genotype with or without the transgene (data not shown). In contrast, genotyping of embryos 18.5 days after coitus from URE-TG^{+}*PU.1*$^{+/-}$ × URE-TG^{-}*PU.1*$^{+/-}$ crosses identified both URE-TG^{+}*PU.1*$^{-/-}$ and URE-TG^{-}*PU.1*$^{-/-}$ animals in the expected Mendelian ratios (data not shown). Importantly, transgenic PU.1 expression led to a partial rescue of granulocytic (Gr1^{+}CD11b^{+}) and monocytic (F4/80^{+}CD11b^{+}) cells to ~ 10% of the numbers detected in *PU.1*$^{+/+}$ control animals (Figure 1B). This confirmed that the transgenes were capable of expressing a functional PU.1 protein. However, quantitative reverse-transcription PCR with RNA from c-kit^{+} progenitors isolated from URE-TG^{+}*PU.1*$^{+/+}$ and URE-TG^{+}*PU.1*$^{-/-}$ fetal livers showed that expression of transgenic PU.1 was 10-fold lower than endogenous levels (Figure 1C). In addition, the transgenes were unable to rescue B-cell development (data not shown). Taken together, these results suggest that the URE alone is insufficient to fully rescue expression in knockout mice and that additional regulatory elements are needed for conferring physiologic PU.1 expression levels in vivo.

A human PU.1 BAC rescues hematopoiesis in *PU.1*$^{-/-}$ mice

We determined the presence of additional *cis*-regulatory elements on the *PU.1* locus by generating transgenic mice carrying a BAC carrying a ~ 179-kb fragment of human chromosome 11 spanning the entire *PU.1* gene locus along with ~ 100 kb 5′ and ~ 50 kb 3′ flanking sequences (GenBank Accession no. AC 074195) (Figure 2A). Because human and mouse *PU.1* genes are highly conserved and to facilitate the structural analysis of transgenes, we used a BAC carrying the human *PU.1* locus and established 2 transgenic lines (#1 and #55). Line #55 contained 3 BAC copies and showed complete integration of the entire BAC, whereas line #1 (2 BAC copies) lacked parts of the 3′ arm (supplemental Figure 1A-B, available on the *Blood* Web site; see the Supplemental Materials link at the top of the online article). All transgenes contained a structurally intact 40-kb central region surrounding the *PU.1* gene (data not shown). These mice were then bred into a *PU.1*$^{+/-}$ background to generate *PU.1*$^{-/-}$ mice with and without the transgene. In the *PU.1*$^{-/-}$ background, both transgenic *PU.1* BAC lines gave rise to viable offspring that were indistinguishable from their *PU.1*$^{+/-}$ littermates and at the expected Mendelian frequencies (Table 1). The rescued knockout animals were fertile, showing that spermatogonial stem cell defects that have been described in *PU.1*$^{-/-}$ mice were also corrected (data not shown).[34]

To analyze mRNA expression from the *PU.1* BAC, we performed quantitative reverse-transcription PCR with species-specific primer/probe sets with equal amplification efficiency (supplemental Figure 2). This showed that the mRNA expression pattern of *PU.1* in both BAC transgenic lines was indistinguishable from that of the endogenous mouse gene in *PU.1*$^{+/+}$ animals, both in tissues and in purified hematopoietic cell populations (Figure 2B-C; data not shown). Next, we assessed human PU.1 protein expression in rescued BAC^{+}*PU.1*$^{-/-}$ mice in total bone marrow (BM) cells, Gr1^{+} granulocytes, CD19^{+} B cells, and BM-derived macrophages by Western blotting and showed levels comparable to those of mouse PU.1 in wild-type control cells (Figure 2D).

The main defect of *PU.1*$^{-/-}$ mice is a complete absence of mature myeloid and B lymphoid cells. To test whether the *PU.1* BAC could rescue formation of these lineages at the correct frequency, we inspected cell composition in the peripheral blood of

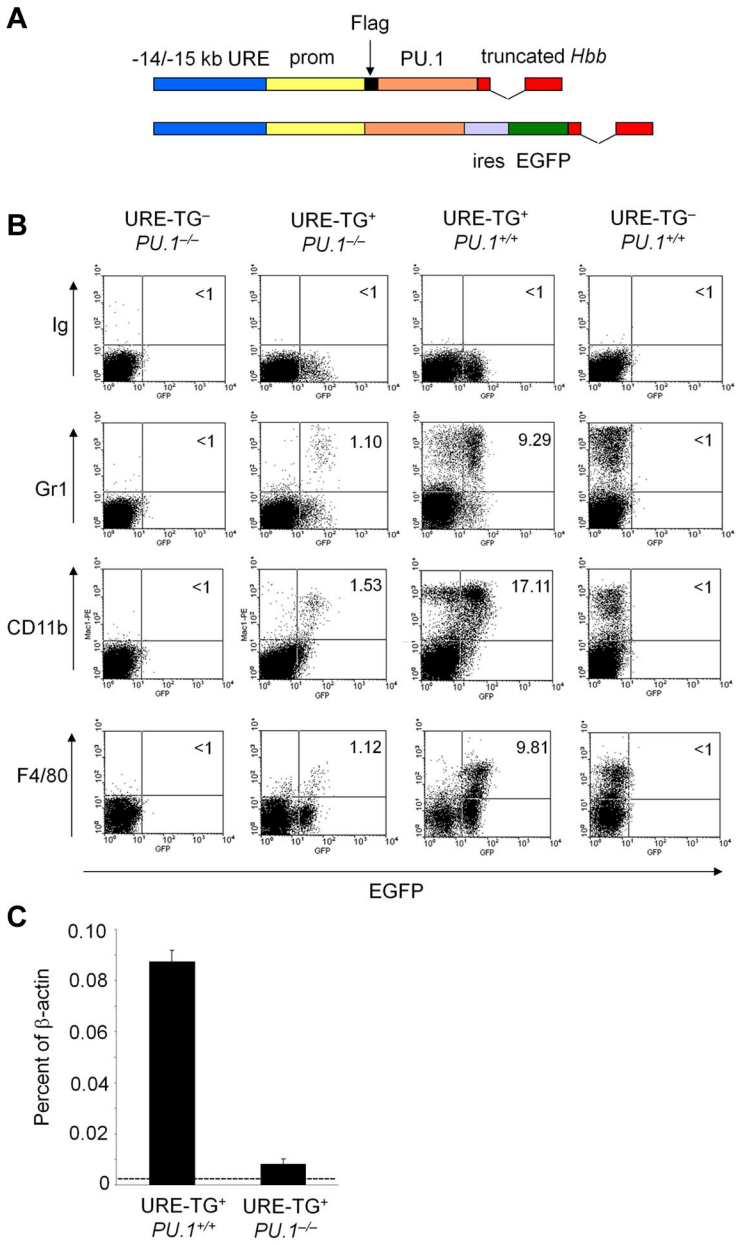

Figure 1. Rescue experiment of *PU.1*$^{-/-}$ hematopoiesis by URE-driven PU.1 cDNA expression. (A) Schematic maps of the URE-based transgenic rescue constructs. A 3.4-kb fragment that included the complete URE was fused to a 2.1-kb proximal *PU.1* promoter fragment and a truncated rabbit *Hbb* gene, providing splicing acceptor/donor sites and a polyA signal as described in "Methods." This plasmid was equipped with the full-length murine PU.1 cDNA that was either fused to a 5′ Flag-tag or a 3′ iresEGFP reporter cassette. (B) Flow cytometry of day 18.5 prenatal fetal liver cell suspensions from the indicated genotypes derived from a PU.1iresEGFP transgenic line. CD11b was used as a pan-myeloid marker, Gr1 was used to detect granulocytes, and F4/80 was used to detect monocytes. Numbers in the upper right quadrates indicate percentages of GFP$^+$ cells carrying the respective myeloid antigenes. The plots are representative of 7 mice each. (C) Real-time RT-PCR with the use of a mouse PU.1-specific primer/probe set and mRNA from c-kit$^+$ fetal liver cells of the indicated mice (n = 3 each) derived from a PU.1iresEGFP transgenic line sorted day 18.5 as template. Data were normalized to the expression of β-actin. Dashed line indicates the qPCR background level detectable in URE-TG$^-$ *PU.1*$^{-/-}$ fetal liver cells.

the transgenic mice and found no significant alterations or morphologic abnormalities compared with age-matched BAC$^-$*PU.1*$^{+/+}$ controls (Table 2; data not shown). Numbers and frequency of monocytes, granulocytes, B cells, and T cells were similar between BAC$^+$*PU.1*$^{-/-}$ and BAC$^-$*PU.1*$^{+/+}$ control mice (Figure 3A-B; supplemental Figure 3). HSCs, myeloid, and megakaryocytic-erythroid progenitors were present in normal frequencies (Figure 3C; data not shown), and BAC$^+$*PU.1*$^{-/-}$ animals formed the same numbers of colonies in response to macrophage colony-stimulating factor (M-CSF) or granulocyte-macrophage colony-stimulating factor as did BAC$^-$*PU.1*$^{+/+}$ control mice (Figure 3D). In contrast, cells from URE$^{-/-}$ mice formed significantly fewer colonies. Morphology and cellular composition of the BAC-rescued colonies were identical to BAC$^-$*PU.1*$^{+/+}$ control colonies (Figure 3E; data not shown). Moreover, the expression of known PU.1 target genes such as *Csf2, Ebf1, IL7r*, and *Csf1r* in BM cells of rescued mice was comparable to that of control mice (Figure 3F).

Together, these experiments confirmed that all regulatory elements required for conferring physiologic PU.1 mRNA and protein expression were located on the BAC and that the human *PU.1* gene is capable of rescuing all aspects of the *PU.1*$^{-/-}$ mouse phenotype.

Genome-scale chromatin structure mapping identifies novel active *cis* elements in the *PU.1* locus

The experiments described above suggested that in addition to the URE other *cis*-regulatory elements were required for high-level PU.1 expression. Active regulatory elements bound by transcription factors exist as DHSs,[35] a feature that has been exploited to identify active *cis* elements. To cover the entire *PU.1* locus and to also verify regulatory principles at global level, we mapped genomewide DHSs in primary macrophages expressing high PU.1 levels and primary B cells expressing intermediate levels.[36] In

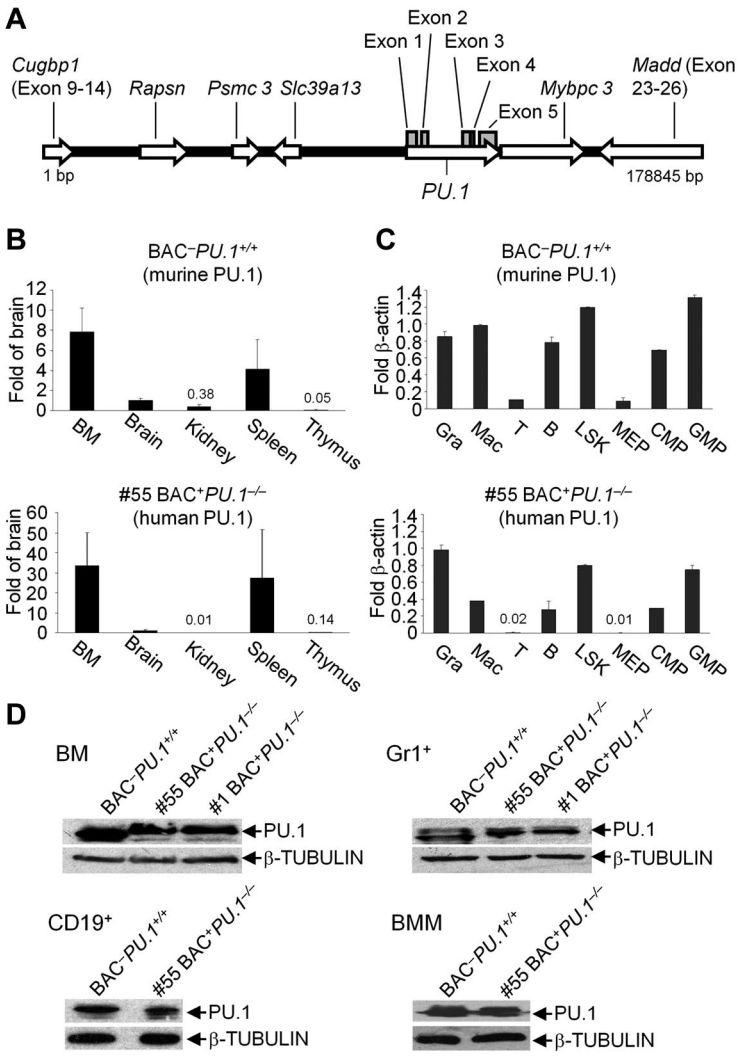

Figure 2. Transgenic expression of the human *PU.1* BAC. (A) Map of the genomic BAC clone containing base pairs 47 499 973 to 47 321 096 of the human chromosome 11. Shown are the positions and orientations (open arrows) of all genes included on the BAC and positions of all *PU.1* exons (gray boxes). (B-C) Comparison of endogenous mouse (top) and transgenic human (bottom) PU.1 transcripts in indicated tissues (B) and hematopoietic cell populations (C) isolated from BAC^{-}*PU.1*$^{+/+}$ and BAC^{+}*PU.1*$^{-/-}$ mice derived from line #55. Shown are quantitative real-time reverse transcription PCR results that represent the mean ± SD of 3 mice per genotype. Data were normalized to the expression of β-actin. BM indicates bone marrow Kid, kidney; Sp, spleen; Thy, thymus. Granulocytes (Gra; Gr1^{+}CD11b^{+}CD19^{-}CD3^{-}), macrophages (Mac; CD11b^{+}Gr1^{-}CD19^{-}CD3^{-}), T cells (CD3^{+}CD19^{-}Gr1^{-}CD11b^{-}), and B cells (CD19^{+}CD3^{-}Gr1^{-}CD11b^{-}) were sorted from spleens, LSK cells (Lin^{-}Sca-1^{+}c-kit^{+}), MEPs (megakaryocyte erythrocyte progenitors; lin^{-}Sca-1^{-}c-kit^{+}CD34^{-}FcγRII/III^{-}), CMPs (common myeloid progenitors; lin^{-}Sca-1^{-}c-kit^{+}CD34^{+}FcγRII/III^{low}), and GMPs (granulocyte monocyte progenitors; lin^{-}Sca-1^{-}c-kit^{+}CD34^{+}FcγRII/III^{+}) were sorted from bone marrow. (D) Western blot analysis showing transgenic human PU.1 protein expression in extracts of total bone marrow (BM) cells (upper left), Gr1^{+}-enriched bone marrow granulocytes (upper right), CD19^{+}-enriched splenic B cells (lower left) and BM-derived macrophages (BMMs; lower right) from BAC^{+}*PU.1*$^{-/-}$ mice of the indicated lines. Total extracts from 10^{6} cells were separated by sodium dodecyl sulfate–polyacrylamide gel electrophoresis, blotted onto a nitrocellulose membrane, and probed with the indicated antibodies.

macrophages, we confirmed the presence of the previously published DHSs at the proximal *PU.1* promoter, in intron 1 and at 14 kb upstream to the *PU.1* gene transcription start site (TSS) (Figure 4A third panel).[15] Our data uncovered several additional DHSs in the *PU.1* locus (designated by their location 5′ of the mouse *PU.1* TSS), a strong DHS at −12 kb and 3 weaker DHSs at −10 kb, −9 kb, and −8 kb. A similar DHS pattern was found in 2 different myeloid cell lines (HPC7 and 416B) with the use of an array-based profiling strategy (supplemental Figure 4A). However, in B cells the DHS pattern was profoundly different, with DHSs at the proximal promoter, in intron 2, and at −14 kb, but not at −12 kb, −10 kb, −9 kb, and −8 kb (Figure 4A bottom). The location of all DHSs coincided with sequence conservation peaks across multiple mammalian genomes (Figure 4A top). This finding showed that differential *PU.1* expression levels in myeloid cells and B cells are associated with marked differences in DHSs.

To further characterize active regulatory elements, we performed ChIP experiments with the use of an antibody against H3K9ac, a modification associated with active chromatin,[37] with the PU.1-expressing myeloid cell lines HPC7 and 416B, as well as with the embryonic stem cell line HM1 and the T-cell line BW5147 as negative controls. Precipitated DNA was hybridized to genomic tiling arrays. In both myeloid lines, we saw strong enrichment of H3K9ac around the *PU.1* TSS, at −15 kb/−14 kb (which comprises the URE) and at −12 kb (Figure 4B). HM1

Table 1. Rescue of the lethal *PU.1*$^{-/-}$ phenotype by transgenic expression of human PU.1

Transgenic line	No. of mice	BAC	Mouse *PU.1* allele +/+	+/−	−/−
#1	137	−	14	37	0
		+	17	50	19
#55	126	−	20	38	0
		+	17	32	19

Genotyping of offspring resulting from mating of BAC^{+}*PU.1*$^{+/-}$ *and BAC*$^{-}$ *PU.1*$^{+/-}$ parents were determined by PCR at weaning.

Table 2. Human PU.1-rescued *PU.1*$^{-/-}$ mice have normal peripheral blood parameters

	BAC^{-}*PU.1*$^{+/+}$	#1 BAC^{+}*PU.1*$^{-/-}$	#55 BAC^{+}*PU.1*$^{-/-}$
White blood cell count, × 10^{3}/mm^{3}	13.06 ± 1.95	10.78 ± 1.26	10.5 ± 1.33
Red blood cell count, × 10^{6}/mm^{3}	12.44 ± 0.76	13.72 ± 4.44	15.1 ± 1.26
Hemoglobin level, g/dL	16.5 ± 0.81	19.2 ± 5.93	10.75 ± 1.73
Lymphocytes, %	72.76 ± 4.88	80 ± 3.25	79.4 ± 4.28
Granulocytes, %	19.66 ± 4.34	13.62 ± 2.9	15.42 ± 3.9
Monocytes, %	7.78 ± 0.93	6.42 ± 1.39	5.66 ± 1.23

Blood was obtained from age-matched mice (12-16 weeks) by tail puncture. Values indicate means ± SDs of the indicated genotypes; n = 5 each.

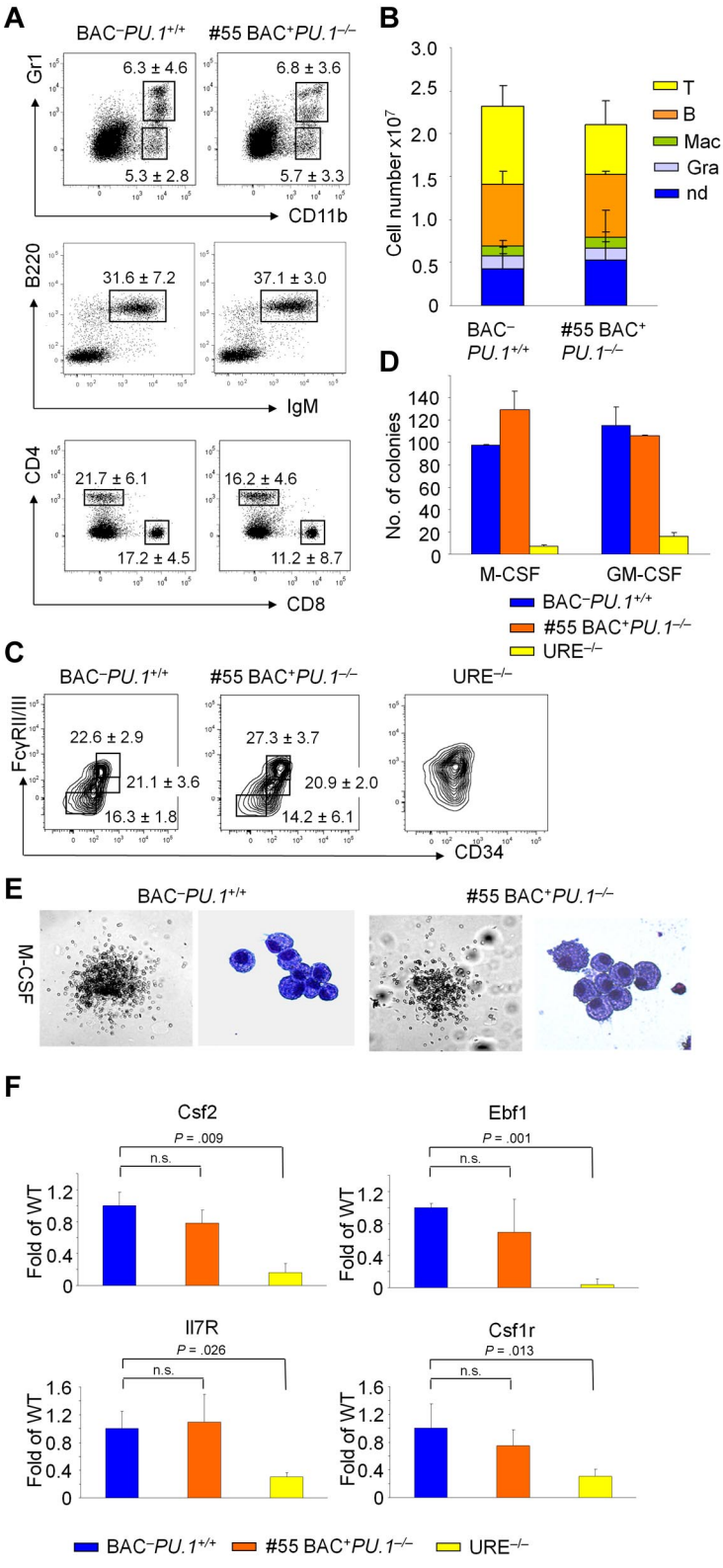

Figure 3. Rescue of *PU.1*$^{-/-}$ hematopoiesis by the *PU.1* BAC. (A) Flow cytometric analysis of splenocytes from indicated mice derived from line #55. Numbers indicate the gated cell means ± SDs in percentage, based on 6 mice per genotype. (B) Total numbers of T cells, B cells, macrophages (Mac), and granulocytes (Gra) in spleens of the mice as analyzed in panel A; nd = not defined. (C) Multiple color flow cytometry showing normal frequencies of GMPs, CMPs, and MEPs. Numbers indicate the gated cell means ± SDs in percentage, based on 3 mice per genotype. A URE$^{-/-}$ mouse is shown for comparison. (D) Myeloid progenitor assay. Total bone marrow cells (1×10^4) from indicated mice were plated in methylcellulose supplemented with M-CSF or granulocyte-macrophage colony-stimulating factor (GM-CSF). Bar graphs show colony numbers scored after 7 days. Cells from URE$^{-/-}$ mice served as a PU.1 low control. (E) Shape of M-CSF–stimulated colonies after 7 days in methylcellulose are shown as phase-contrast images. Cellular morphology is shown by May-Grünwald-Giemsa stains. (F) Real-time reverse transcription PCR, showing expression of indicated PU.1 target genes in bone marrow cells. mRNA from the bone marrow of URE$^{-/-}$ mice was used as a PU.1 low control; n.s. indicates not significant.

and BW5147 cells showed no or very weak H3K9ac at these sites. We further corroborated the myeloid-specific H3K9ac pattern by ChIP– quantitative PCR (qPCR; supplemental Figure 4B). The same regions that carried H3K9ac also carried dimethylated H3K4 as another modification associated with active chromatin (supplemental Figure 5).

Finally, with the use of a publically available ChIP-sequencing library prepared from mouse macrophages,[29] we found that the −14-kb, −12-kb, and −10-kb sites were strongly bound by the histone acetyltransferase p300, which has been shown to mark active enhancer elements (Figure 4C).[38,39] Taken together, our chromatin structure profiling allowed us to delineate additional candidate distal regulatory

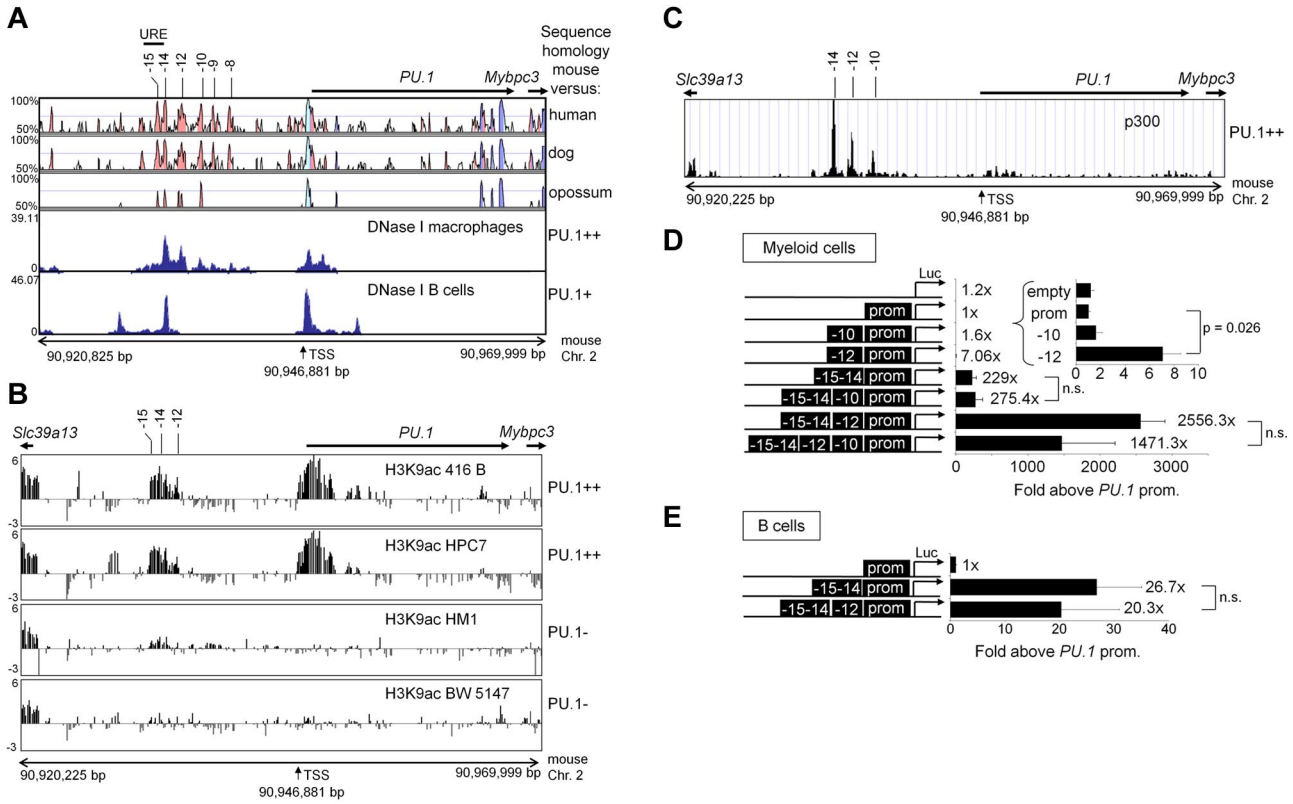

Figure 4. Synergism between *PU.1* gene distal *cis* elements. (A) The top part shows a MVista representation of sequence conservation across ~ 50 kb of the region of mouse chromosome 2 that harbors the *PU.1* locus. The conservation panels correspond to, from top to bottom, mouse/human, mouse/dog, and mouse/opossum alignments. The conservation plots show regions with ≥ 50% of conservation (indicated on the y-axis). Exons are shown in blue, noncoding conserved regions in pink. Positions of nonconserved sequence homology regions are indicated. Precise locations of the previously unidentified homology regions are −12 kb = 12.3 kb, −10 kb = 10.5 kb, −9 kb = 9.5 kb, and −8 kb = 7.8 kb upstream of the *PU.1* TSS. The bottom part shows a University of California Santa Cruz (UCSC) genome browser screenshot of DNaseI hypersensitivity site sequencing profiles across the mouse *PU.1* locus in bone marrow–derived macrophages and splenic B cells. Relative enrichments are indicated at the y-axes; ++ and + on the right indicates strong or intermediate PU.1 expression, respectively. (B) ChIP-chip mapping of H3K9ac across the murine *PU.1* locus with the use of custom-designed genomic tiling arrays. The y-axis represents the log 2 enrichment of ChIPed DNA over input DNA, whereas the x-axis depicts 50-kb genomic sequence spanning the mouse *PU.1* locus. At the top, positions of the indicated DHSs and the covered genes are marked. The genomic coordinates (in base pairs) of mouse chromosome 2 covered on the array are shown at the bottom. (C) Raw p300 ChIP-sequencing data across the murine *PU.1* locus in bone marrow–derived macrophages showing p300 occupancy exclusively at the indicated DHSs. (D) Luciferase activity assay of RAW264.7 macrophages stably transfected with the indicated constructs. Multiple independent clones were assayed for each construct, and luciferase activity was normalized to the plasmid copy number as determined by Southern blotting. Shown are the means ± SDs of ≥ 6 independent clones for each construct. The average activity of the *PU.1* promoter only construct was set to 1. The inlet shows a higher magnification of the values of the indicated constructs; n.s. indicates not significant. (E) Luciferase activity assay of Namalwa B cells stably transfected with the indicated constructs. Shown are the mean ± SD of 3 independent cell pools for each construct.

elements associated with high-level expression of the *PU.1* gene in myeloid cells.

Functional synergism between *PU.1* gene distal regulatory elements in a chromatin context

We next tested the novel candidate *PU.1* regulatory elements for their chromatin activation abilities with the use of reporter assays in stably transfected cell lines and examined a series of constructs in which a luciferase gene was driven by a 0.5-kb minimal *PU.1* promoter along with the −15 kb/−14 kb DHSs (URE), the −12-kb DHS, or the −10-kb DHS either alone or in combinations. We electroporated linearized constructs into the RAW264.7 macrophage cell line and the Namalwa B-cell line and determined the copy numbers of integrated plasmids in individual puromycin-resistant clones or cell pools or both (data not shown). In myeloid cells and in line with our previously published results,[15] the *PU.1* promoter alone was unable to drive reporter activity above background levels, whereas the addition of the URE had a profound enhancing effect (Figure 4D). Although to a lesser extent, −12 kb DHS also enhanced reporter gene activity. However, the addition of the URE and −12-kb DHS together boosted reporter gene activity to a value of nearly 10-fold above that of the URE alone. In contrast, the −10-kb DHS, alone or in combination with the URE and the −12 kb DHS, showed no enhancer activity. The situation in B cells was different. Here, the addition of the −12-kb DHS to the URE did not enhance reporter gene activity over that of the URE alone (Figure 4E).

Collectively, these results identify the −12-kb DHS as a *cis* element that cooperates with the URE to drive high-level *PU.1* promoter activity within the chromatin of myeloid cells but not B lymphocytes.

Myeloid-specific PU.1 auto-activation is required for −12-kb enhancer function

The −12-kb DHS contains a highly conserved PU.1 consensus sequence (Figure 5A).[40] To test for specific PU.1 binding in the −12-kb DHS, we performed gel shift experiments with a probe spanning the predicted PU.1 site (Figure 5B). We detected a single major band that was present in nuclear extracts from RAW264.7 macrophages but not NIH-3T3 fibroblasts. The identity of this band as PU.1 was confirmed by probe competition and a supershift with an anti-PU.1 antibody. Myeloid-specific binding of PU.1 to the

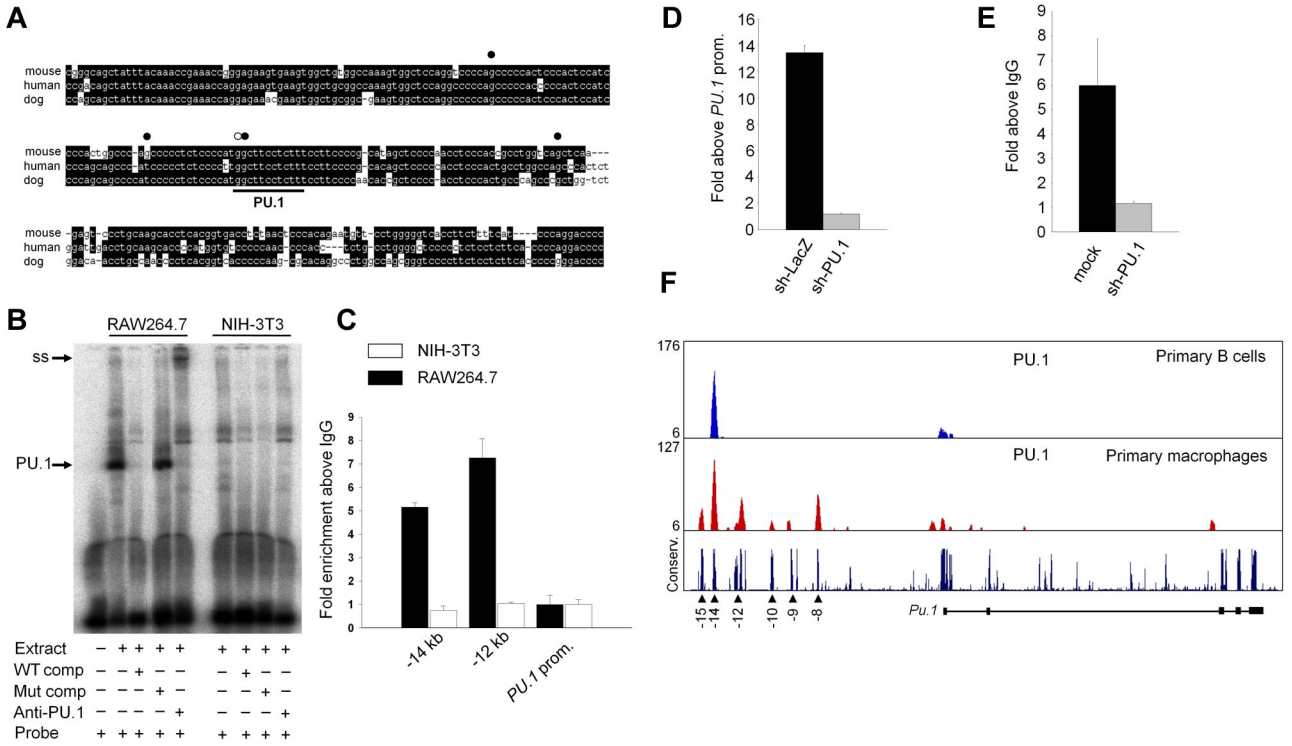

Figure 5. Myeloid-specific PU.1 autoregulation at the −12-kb element. (A) Sequence alignment of the −12-kb DHS of mouse, human, and dog. Identical residues are shown in black. The PU.1 binding motifs as identified by rVista software and the dimethylsulfate footprinting pattern obtained with macrophages (see supplemental Figure 6) are indicated. (B) Electromobility shift assay showing PU.1 binding to the −12-kb DHS. Nuclear extracts from RAW264.7 macrophages (left) and NIH-3T3 fibroblasts (right) were incubated with a ^{32}P-labeled probe containing the potential PU.1 binding site of the −12-kb DHS, as well as an antibody to PU.1 and unlabeled competitor oligonucleotides, as indicated. Base pair exchanges from ga*ggaa*gc to ga*gcgc*gc in the PU.1 motif are indicated (mut). The position of PU.1 and a supershift complex (ss) are shown. (C) ChIP-qPCR showing strong PU.1 in vivo binding to the −12-kb DHS in RAW264.7 macrophages but not in 3T3-NIH fibroblasts. Binding to the −14-kb element and the proximal promoter are shown as controls. The values were normalized to a ChIP with the use of an IgG-control antibody. (D) Reporter assay data with RAW264.7 cells stably carrying a −12-kb DHS-driven luciferase construct. The cells were transiently transfected with constructs expressing shRNAs against either PU.1 or the LacZ gene, as a control, along with a GFP marker to allow flow cytometric sorting of the transfected cells. The values are normalized to luciferase activities driven by *PU.1* promoter alone. (E) ChIP-qPCR with RAW264.7 cells that were untreated (mock) or were stably transfected with a shRNA against PU.1 showing reduced H3K9ac at the −12-kb region after PU.1 knockdown. The values are normalized to a ChIP with an IgG-control antibody. (F) UCSC Genome browser representation of PU.1 occupancy at the *PU.1* locus in mouse peritoneal macrophages and splenic CD19$^+$ B cells as shown by ChIP-seq tag counts ($\log_2$).

−12-kb enhancer in vivo was confirmed by ChIP experiments (Figure 5C) which showed strong PU.1 binding specifically to the −12-kb DHS and the −14-kb URE region. The same site was found to be occupied in in vivo dimethylsulfate footprinting experiments (supplemental Figure 6). This assay also showed additional myeloid-specific footprints, indicating that the −12-kb DHS was occupied by several factors.

We depleted PU.1 by shRNA-mediated knockdown in RAW264.7 macrophages stably carrying the −12-kb enhancer-driven luciferase construct. This showed that PU.1 was crucial for its activity (Figure 5D; supplemental Figure 7). Furthermore, PU.1 knockdown led to a decrease in H3K9ac at the −12-kb region, indicating that PU.1 was necessary for the local assembly of transcriptionally active chromatin (Figure 5E).

We next compared our DNaseI-seq data with ChIP-sequencing data[28] to examine PU.1 binding across its entire locus in macrophages and B cells and uncovered a PU.1-binding pattern in macrophages that overlapped almost completely with all previously identified DHSs (Figure 5F). PU.1 binding was strong at positions −14 kb, −12 kb, and −8 kb and was weaker but detectable at −15 kb, −10 kb, −9 kb, and at the proximal promoter. PU.1 binding was markedly more restricted in B cells, with strong binding at position −14 kb and weak binding at the promoter, but not anywhere else in the locus. Differential binding of PU.1 to the −12-kb region was confirmed by ChIP-qPCR (data not shown). These data indicated that high-level PU.1 expression in myeloid cells is driven by a cell type–specific PU.1 auto-regulatory loop that involves all distal *cis*-regulatory elements.

PU.1 chromatin entry at the −12-kb enhancer requires C/EBPα binding to the URE

We next asked why PU.1 could bind the URE in both myeloid cells and B cells but bound the −12-kb element exclusively in myeloid cells. We addressed this question by searching our genomewide DHS-seq data for common transcription factor–binding motifs associated with open chromatin regions. This showed 58 628 DHSs in macrophages and 72 959 DHSs in B cells; 43.5% of the macrophage and 54.6% of the B-cell DHSs were unique for the respective cell types (Figure 6A); 35.9% of the unique macrophage, 14.5% of the unique B cell, and 11.4% of the common DHSs were bound by PU.1, suggesting that PU.1 occupancy is linked to open chromatin, particularly in macrophages (Figure 6B). Further separation of the PU.1-bound DHSs according to their genomic coordinates showed that the cell type–specific differences in PU.1 occupancies were located mainly in promoter-distal regions (Figure 6C; supplemental Figure 8).

To examine which transcription factor binding motifs were associated with PU.1-bound regions of open chromatin we performed de novo motif analysis as described (supplemental Figure 9).[28] No particular preferences for B cell– and myeloid-specific factor binding motifs were found in promoter-distal DHSs common

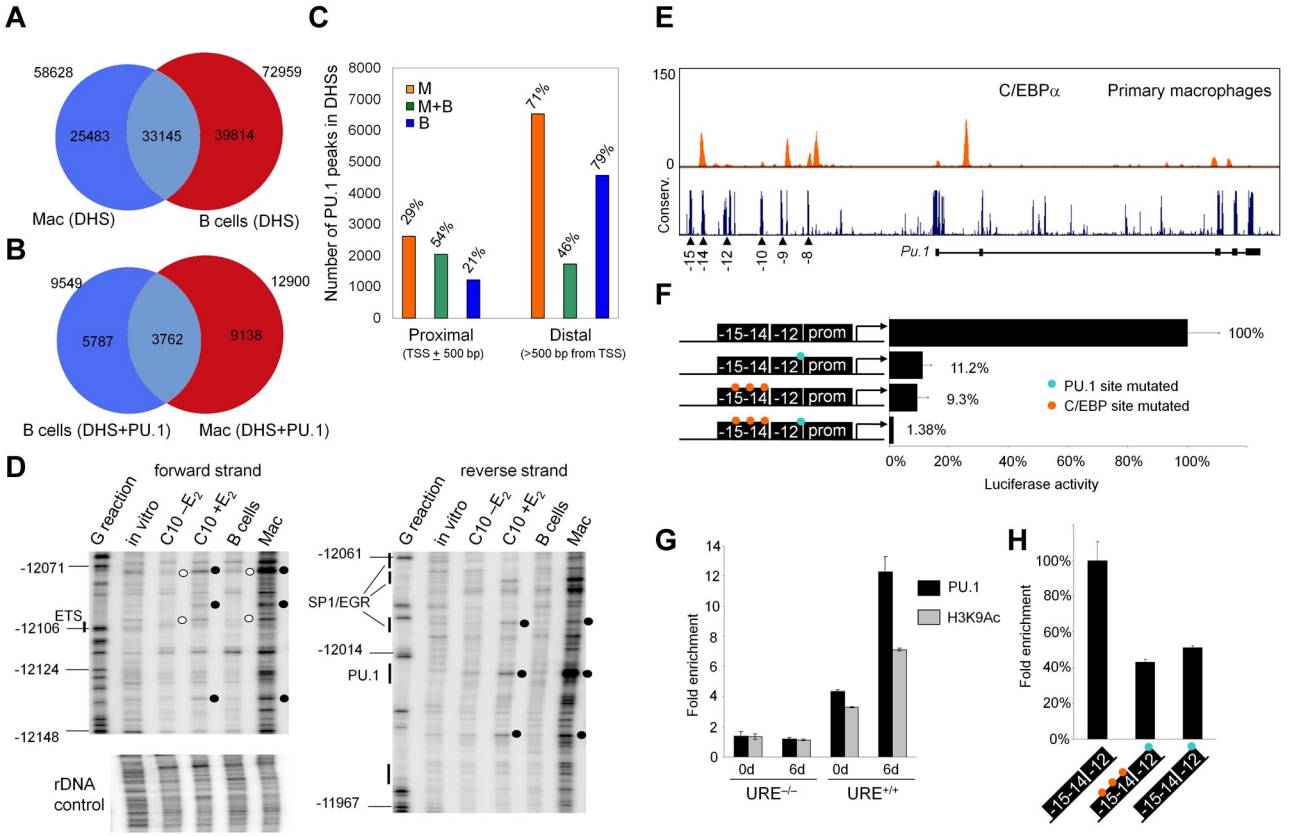

Figure 6. The −12-kb enhancer requires C/EBPα and cross-interaction with the URE. (A) Venn diagram showing the global numbers of DHSs in macrophages and B cells. The condition for peak overlap was that center of the peak in the first dataset should lie within boundaries of a peak in the second dataset. (B) Numbers of PU.1-occupied DHSs in macrophages and B cells. Peak identification in panels A and B used a false discovery threshold of 0.1%. (C) Total number of PU.1-occupied DHSs unique to macrophages, unique to B cells, or common to both cell types found in promoter-proximal (within ± 500 bp from TSS) and distal (> 500 bp from TSS) genomic regions. (D) DNaseI in vivo footprinting of the −12-kb enhancer in C10 cells before ($-E_2$) or after ($+E_2$) 72 hours of β-estradiol induction, B cell, and macrophages. In vitro DNaseI-treated DNA served as a control, and a G-reaction was used to indicate genomic positions relative to the TSS. Samples were assayed with forward (left) and reverse (right) primers for the −12-kb enhancer, as well as with primers for the rDNA genes to control for equal digestion. Hyperreactivities are marked by closed circles and protections by open circles. (E) UCSC Genome browser image depicting C/EBPα ChIP-seq tag counts (normalized to 10^7 sequence tags) ($\log_2$) at the *PU.1* locus in macrophages and B cells. (F) Luciferase assay in RAW264.7 macrophages stably transfected with the indicated constructs. Mutations in PU.1-binding motifs are indicated by blue or orange dots, respectively. Shown are the mean values ± SDs of 3 independent cell bulks for each construct. Activity of the wild-type construct was set as 100%. (G) ChIP-qPCRs at the −12-kb DHS in URE$^{-/-}$ and URE$^{+/+}$ myeloid cell lines (see "Methods") after retroviral transduction with a tamoxifen-responsive C/EBPα construct. Shown is PU.1 occupancy (black bars) and H3K9ac (gray bars) before and after 6 days of tamoxifen induction. (H) ChIP-qPCRs depicting H3K9ac levels at the exogenous −12-kb DHS of the indicated constructs in stably transfected RAW264.7 cells. Blue dots indicate mutation in PU.1 binding site; orange dots, mutation in C/EBP binding site. All values were normalized to integrated plasmid copy numbers.

to both cell types. However, AP1 and C/EBP-binding motifs were among the main PU.1-associated sequences in promoter-distal DHSs of macrophages, whereas in distal elements of B cells PU.1 was associated with motifs for B cell–specific factors such as EBF and E2A. C/EBPα is the major family member expressed in myeloid cells, is not expressed in B cells, and can up-regulate *PU.1* transcription.[41] Moreover, it is capable of reprogramming B cells into macrophages on its ectopic activation.[42] To examine whether C/EBPα can instruct the activation of the chromatin at the −12-kb enhancer, we performed in vivo DNaseI footprinting and ChIP experiments with the use of a B cell to macrophage reprogramming system that is based on a B-cell line carrying an estrogen-responsive C/EBPα transgene.[19] Expression of C/EBPα led to the activation of this element as indicated by a switch of the DNaseI accessibility pattern from that of B cells to that of macrophages, an increase in PU.1 occupancy, and enhanced H3K9ac (Figure 6D; supplemental Figure 10A-C).

However, ChIP-seq experiments[28] did not detect C/EBPα or C/EBPβ binding at the −12-kb DHS but only at the −14-kb URE and 3 additional sites in the *PU.1* locus (Figure 6E; data not shown). Moreover, the comparison of ChIP- and DHS-sequencing data showed that C/EBPα occupied 38.9% (= 3186) of the promoter-distal DHSs together with PU.1 in macrophages, indicating that at the global level many, but not all, PU.1-occupied DHSs are co-occupied by C/EBPα (data not shown). Together, these findings suggested that C/EBPα activated the −12-kb enhancer indirectly by binding to other regulatory elements such as the URE. Indeed, mutation of the 3 C/EBP sites in the URE (and/or the PU.1 site in the −12-kb DHS) within a URE/−12-kb DHS-driven luciferase construct led to profoundly reduced reporter activity in stable transfectants (Figure 6F). Furthermore, retrovirally transduced C/EBPα failed to induce PU.1 binding and promotion of H3K9ac at the −12-kb element in myeloid cells derived from a URE$^{-/-}$ mouse (Figure 6G). Finally, mutation of the URE C/EBPα sites decreased H3K9ac at the −12-kb region to the same extent as mutation of the −12-kb DHS PU.1 site in constructs stably integrated in the chromatin of transfected RAW264.7 cells (Figure 6H).

Taken together, these experiments indicate that (1) the URE regulates chromatin activation of the −12-kb enhancer in myeloid but not in B cells, (2) PU.1 can only access its binding site at the −12-kb element in myeloid cells, and (3) binding of C/EBPα to the URE in myeloid cells prepares the −12-kb

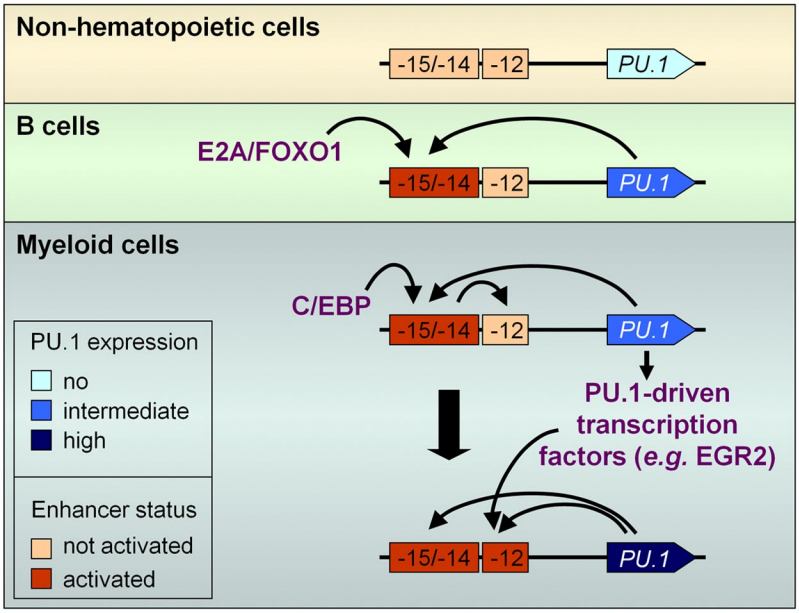

Figure 7. Regulated interaction between *cis*-regulatory elements orchestrates the PU.1 expression pattern. Lack of PU.1 expression in nonhematopoietic cells is due to the lack of activation of critical enhancer elements located upstream of the *PU.1* gene. The intermediate PU.1 levels expressed in B cells are driven by the assembly of a B cell–specific transcription factor complex at the −14-kb URE, which includes E2A and FOXO1, and the formation of a PU.1 autoregulatory loop. However, this complex is obviously not able to activate additional *cis* elements in the *PU.1* locus. In contrast, myeloid progenitors express C/EBPα which binds the URE, induces the activation of the −12-kb enhancer to allow formation of a second PU.1 autoregulatory loop and binding of additional PU.1-driven transcription factors, such as EGR2, to increase PU.1 expression levels. Black arrows indicate transcription factor interactions/noncoding RNA; red arrows, enhancer-promoter interactions.

enhancer for autoregulatory PU.1 chromatin entry. Importantly, the genomewide data on open chromatin regions and PU.1- and C/EBPα-occupancy patterns in macrophages and B cells suggest that similar regulatory principles apply at the global level.

Discussion

Correct regulation of *PU.1* in mice requires the interaction of multiple elements

Our previous studies have shown that the absence of the URE affects expression of *PU.1* in all PU.1-expressing cell types, indicating that it acts as a general *cis*-regulatory element able to function in different hematopoietic lineages.[13] Our experiments provide clear evidence for the notion that the URE, although crucial for *PU.1* activation in all cell types, is not sufficient for high-level gene expression and has to interact with other elements for correct regulation to occur. We used genomewide DHS maps to identify a new cluster of distal potential *PU.1* regulator elements and show that the number and position of these DHSs is profoundly different in macrophages and B cells. A similar DHS pattern in the myeloid *PU.1* locus was found with the use of a manual mapping approach.[43] The only *PU.1* promoter-distal DHS common to macrophages and B cells locates to the −14-kb URE, further supporting the notion that this region has a general role in PU.1 regulation. Our molecular characterization identified a novel enhancer element at −12 kb that strongly synergizes with the URE to efficiently remodel chromatin and mediates high-level gene expression. The addition of additional DHS-harboring sequences did not significantly increase reporter gene activity in a chromatin context, indicating that most of the transcriptional enhancer and chromatin activation activity at *PU.1* is shared between these 2 elements.

Autoregulation is a common mechanism to adjust the expression of many transcription factors during cellular differentiation.[44-46] PU.1 positively autoregulates its own expression by binding to the −14-kb URE.[16] The −12-kb enhancer also binds PU.1, and we show that this is crucial for enhancer activity. In addition, PU.1 is required to maintain an active chromatin structure at this element. This is in contrast to the URE that is capable of maintaining active chromatin in the absence of PU.1 and that is activated by factors acting early in blood cell development, such as RUNX1,[47,48] suggesting that the 2 elements are hierarchically regulated and may be activated at different stages in development.

The mechanism of −12-kb enhancer element activation involves cross talk with the URE

Our data prompted the question of what activated the −12-kb region exclusively in myeloid cells but not in B cells. The most probable possibility was that myeloid-restricted transcription factors with chromatin remodeling capability were being recruited to the −12-kb region. Indeed, expression of C/EBPα led to chromatin reorganization and PU.1 binding at the −12-kb element. However, chromatin activation at the −12-kb enhancer required the adjacent −14-kb URE region, and C/EBPα did not bind the −12-kb element but instead bound to the URE as has previously been shown.[23] Taken together, this indicates a mechanism in which C/EBP binding to the URE opens the −12-kb region to permit PU.1 auto-activation in myeloid cells (Figure 7). A possible mechanism to achieve this would involve a role for noncoding RNAs that are launched from the URE toward the proximal *PU.1* promoter.[48] An additional, not mutually exclusive mechanism could be that factors induced by high levels of PU.1 in myeloid cells, such as early growth response 2 (EGR2),[49] cooperate with PU.1 at the −12-kb enhancer. In this model, the absence of the URE would reduce PU.1 levels below the threshold for their induction. We have indeed been able to show that the induction of PU.1 leads to an association of EGR2 with this element (data not shown).

The URE is activated by RUNX1 early in development, but once other factors become up-regulated during hematopoietic development, such as C/EBPα, RUNX1 is not required anymore for maintaining active chromatin at this element.[47] Because B cells do not express C/EBPα, this prompted the question as to which factors cooperate with PU.1 to maintain active chromatin at the URE in B cells. Recent high-throughput studies in B cells show that the URE, but not the −12-kb enhancer, is bound by B cell–specific factors such as E2A and FOXO1, in addition to PU.1[50]

(data not shown), suggesting that PU.1 cooperates with different factors to maintain an open chromatin structure in B cells and macrophages (Figure 7).

PU.1 binding and open chromatin

The comparison of global DHS and ChIP data showed that PU.1 occupancy had a stronger association with open chromatin regions in macrophages than in B cells. C/EBP-binding motifs were among the main PU.1-associated sequences in promoter-distal DHSs in macrophage chromatin, and half of these DHSs were co-occupied by C/EBP factors. However, the other half lacked C/EBP sites, indicating that PU.1 binding does not generally require the simultaneous binding of C/EBP. Our finding that C/EBPα could activate the −12-kb enhancer by binding to the URE indicates that at least some of these sites could be subject to a similar mechanism of *cis*-element cross talk and hierarchical regulation.

Our data comparison also confirms that distal regulatory regions harboring open chromatin in B cells and binding PU.1 are enriched for motifs for B cell–specific factors and that *cis*-regulatory elements common to both B cells and macrophages are mainly associated with promoters.[28] However, the URE belongs to a class of distal elements capable of maintaining open chromatin in various cell types by binding alternate tissue-specific factor combinations (as shown here for C/EBPα and E2A/FOXO1). We did not detect a significant enrichment of B cell– or macrophage–specific factor binding motifs associating with PU.1-bound distal DHSs common to B cells and macrophages. Within the myeloid lineage, *PU.1* is expressed also in mast cells, which are regulated by a different transcription factor network, and express, for example, GATA 2.[51] How the *PU.1* URE is regulated in these cells is not known, but our genomewide data suggest that, depending on in how many tissues such specialist elements are active, it is probable that they use variable combinations of transcription factors to maintain activity. It is therefore necessary to first unravel such interactions by detailed analysis of specific genes before embarking on global studies. The *PU.1* URE therefore serves as an important paradigm of how *cis*-regulatory elements use different combinations of tissue-specific factors to maintain expression in different cell types and at different levels.

Acknowledgments

We thank J. F. Zinke, V. Malchin, N. Endruhn, and K. Wronski for technical assistance; B. Jerchow for injection of the transgenic constructs; R. Auburn for printing the custom arrays; T. Graf for C10 cells; J. Cammenga for the inducible C/EBPα retroviral construct; G. Taylor and J. Morgan for high-throughput sequencing; and P. N. Cockerill giving suggestions.

This work was supported by grants from the German Research Foundation (DFG) and the Helmholtz Association of German Research Centers (HGF) (F.R.), the Biotechnology and Biological Sciences Research Council (BBSRC), the Candlelighter's and the Leukemia and Lymphoma Research (C.B.), and the National Institutes of Health (NIH R01 CA41456) (D.G.T.).

Authorship

Contribution: M.L., C.P., M.H., S.G., S.H., N.K.W., G.F., J.S., L.V., and F.R. conducted experiments; F.R. and C.B. wrote the manuscript; M.L. generated figures; D.G.T. and B.G. provided ideas and essential experimental support; C.B. and F.R. designed and supervised the project; A.M.M., S.A., W.C., and D.R.W. performed computational analyses.

Conflict-of-interest disclosure: The authors declare no competing financial interests.

The current affiliation for A.M.M. is Department of Statistics, University of Zanjan, Zanjan, Iran.

Correspondence: Frank Rosenbauer, Max Delbrück Center for Molecular Medicine Robert-Rössle-Strasse 10, 13125 Berlin, Germany; e-mail: f.rosenbauer@mdc-berlin.de; and Constanze Bonifer, Leeds Institute of Molecular Medicine University of Leeds, St James's University Hospital Leeds LS9 7TF, United Kingdom; e-mail: c.bonifer@leeds.ac.uk

References

1. Klemsz MJ, McKercher SR, Celada A, van Beveren C, Maki RA. The macrophage and B cell-specific transcription factor PU.1 is related to the ets oncogene. *Cell.* 1990;61(1):113-124.
2. Scott EW, Simon MC, Anastasi J, Singh H. Requirement of transcription factor PU.1 in the development of multiple hematopoietic lineages. *Science.* 1994;265(5178):1573-1577.
3. McKercher SR, Torbett BE, Anderson KL, et al. Targeted disruption of the PU.1 gene results in multiple hematopoietic abnormalities. *EMBO J.* 1996;15(20):5647-5658.
4. Iwasaki H, Somoza C, Shigematsu H, et al. Distinctive and indispensable roles of PU.1 in maintenance of hematopoietic stem cells and their differentiation. *Blood.* 2005;106(5):1590-1600.
5. Dakic A, Metcalf D, Di RL, et al. PU.1 regulates the commitment of adult hematopoietic progenitors and restricts granulopoiesis. *J Exp Med.* 2005;201(9):1487-1502.
6. Dahl R, Walsh JC, Lancki D, et al. Regulation of macrophage and neutrophil cell fates by the PU.1:C/EBPalpha ratio and granulocyte colony-stimulating factor. *Nat Immunol.* 2003;4(10):1029-1036.
7. Bakri Y, Sarrazin S, Mayer UP, et al. Balance of MafB and PU.1 specifies alternative macrophage or dendritic cell fate. *Blood.* 2005(7);105:2707-2716.
8. Carotta S, Dakic A, D'Amico A, et al. The transcription factor PU.1 controls dendritic cell development and Flt3 cytokine receptor expression in a dose-dependent manner. *Immunity.* 2010;32(5):628-641.
9. Rosenbauer F, Wagner K, Kutok JL, et al. Acute myeloid leukemia induced by graded reduction of a lineage-specific transcription factor, PU.1. *Nat Genet.* 2004;36(6):624-630.
10. Metcalf D, Dakic A, Mifsud S, et al. Inactivation of PU.1 in adult mice leads to the development of myeloid leukemia. *Proc Natl Acad Sci U S A.* 2006;103(5):1486-1491.
11. Cook WD, McCaw BJ, Herring C, et al. PU.1 is a suppressor of myeloid leukemia, inactivated in mice by gene deletion and mutation of its DNA binding domain. *Blood.* 2004;104(12):3437-3444.
12. Moreau-Gachelin F, Tavitian A, Tambourin P. Spi-1 is a putative oncogene in virally induced murine erythroleukaemias. *Nature.* 1988;331(6153):277-280.
13. Rosenbauer F, Owens BM, Yu L, et al. Lymphoid cell growth and transformation are suppressed by a key regulatory element of the gene encoding PU.1. *Nat Genet.* 2006;38(1):27-37.
14. Anderson MK, Weiss AH, Hernandez-Hoyos G, Dionne CJ, Rothenberg EV. Constitutive expression of PU.1 in fetal hematopoietic progenitors blocks T cell development at the pro-T cell stage. *Immunity.* 2002;16(2):285-296.
15. Li Y, Okuno Y, Zhang P, et al. Regulation of the PU.1 gene by distal elements. *Blood.* 2001;98(10):2958-2965.
16. Okuno Y, Huang G, Rosenbauer F, et al. Potential autoregulation of transcription factor PU.1 by an upstream regulatory element. *Mol Cell Biol.* 2005;25(7):2832-2845.
17. Smith AM, Sanchez MJ, Follows GA, et al. A novel mode of enhancer evolution: the Tal1 stem cell enhancer recruited a MIR element to specifically boost its activity. *Genome Res.* 2008;18(9):1422-1432.
18. Pinto do OP, Kolterud A, Carlsson L. Expression of the LIM-homeobox gene LH2 generates immortalized steel factor-dependent multipotent hematopoietic precursors. *EMBO J.* 1998;17(19):5744-5756.
19. Bussmann LH, Schubert A, Vu Manh TP, et al. A robust and highly efficient immune cell reprogramming system. *Cell Stem Cell.* 2009;5(5):554-566.
20. Akashi K, Traver D, Miyamoto T, Weissman IL. A clonogenic common myeloid progenitor that gives rise to all myeloid lineages. *Nature.* 2000;404(6774):193-197.

21. Landry JR, Bonadies N, Kinston S, et al. Expression of the leukemia oncogene Lmo2 is controlled by an array of tissue-specific elements dispersed over 100 kb and bound by Tal1/Lmo2, Ets, and Gata factors. *Blood.* 2009;113(23):5783-5792.
22. Follows GA, Dhami P, Gottgens B, et al. Identifying gene regulatory elements by genomic microarray mapping of DNaseI hypersensitive sites. *Genome Res.* 2006;16(10):1310-1319.
23. Yeamans C, Wang D, Paz-Priel I, et al. C/EBPalpha binds and activates the PU.1 distal enhancer to induce monocyte lineage commitment. *Blood.* 2007;110(9):3136-3142.
24. Lefevre P, Lacroix C, Tagoh H, et al. Differentiation-dependent alterations in histone methylation and chromatin architecture at the inducible chicken lysozyme gene. *J Biol Chem.* 2005; 280(30):27552-27560.
25. Lausen J, Liu S, Fliegauf M, Lubbert M, Werner MH. ELA2 is regulated by hematopoietic transcription factors, but not repressed by AML1-ETO. *Oncogene.* 2005;25(9):1349-1357.
26. Tagoh H, Himes R, Clarke D, et al. Transcription factor complex formation and chromatin fine structure alterations at the murine c-fms (CSF-1 receptor) locus during maturation of myeloid precursor cells. *Genes Dev.* 2002;16(13):1721-1737.
27. Walter K, Bonifer C, Tagoh H. Stem cell-specific epigenetic priming and B cell-specific transcriptional activation at the mouse Cd19 locus. *Blood.* 2008;112(5):1673-1682.
28. Heinz S, Benner C, Spann N, et al. Simple combinations of lineage-determining transcription factors prime cis-regulatory elements required for macrophage and B cell identities. *Mol Cell.* 2010; 38(4):576-589.
29. Ghisletti S, Barozzi I, Mietton F, et al. Identification and characterization of enhancers controlling the inflammatory gene expression program in macrophages. *Immunity.* 2010;32(3):317-328.
30. Li H, Ruan J, Durbin R. Mapping short DNA sequencing reads and calling variants using mapping quality scores. *Genome Res.* 2008;18(11): 1851-1858.
31. Fejes AP, Robertson G, Bilenky M, et al. FindPeaks 3.1: a tool for identifying areas of enrichment from massively parallel short-read sequencing technology. *Bioinformatics.* 2008;24(15): 1729-1730.
32. Mahony S, Benos PV. STAMP: a web tool for exploring DNA-binding motif similarities. *Nucleic Acids Res.* 2007;35(Web Server issue):W253-W258.
33. Broske AM, Vockentanz L, Kharazi S, et al. DNA methylation protects hematopoietic stem cell multipotency from myeloerythroid restriction. *Nat Genet.* 2009;41(11):1207-1215.
34. Olive V, Wagner N, Chan S, et al. PU.1 (Sfpi1), a pleiotropic regulator expressed from the first embryonic stages with a crucial function in germinal progenitors. *Development.* 2007;134(21):3815-3825.
35. Gross DS, Garrard WT. Nuclease hypersensitive sites in chromatin. *Annu Rev Biochem.* 1988;57: 159-197.
36. Nutt SL, Metcalf D, D'Amico A, Polli M, Wu L. Dynamic regulation of PU.1 expression in multipotent hematopoietic progenitors. *J Exp Med.* 2005; 201(2):221-231.
37. Koch CM, Andrews RM, Flicek P, et al. The landscape of histone modifications across 1% of the human genome in five human cell lines. *Genome Res.* 2007;17(6):691-707.
38. Heintzman ND, Stuart RK, Hon G, et al. Distinct and predictive chromatin signatures of transcriptional promoters and enhancers in the human genome. *Nat Genet.* 2007;39(3):311-318.
39. Visel A, Rubin EM, Pennacchio LA. Genomic views of distant-acting enhancers. *Nature.* 2009; 461(7261):199-205.
40. Friedman AD. Transcriptional regulation of granulocyte and monocyte development. *Oncogene.* 2002;21(21):3377-3390.
41. Friedman AD. Transcriptional regulation of myelopoiesis. *Int J Hematol.* 2002;75(5):466-472.
42. Xie H, Ye M, Feng R, Graf T. Stepwise reprogramming of B cells into macrophages. *Cell.* 2004;117(5):663-676.
43. Zarnegar MA, Chen J, Rothenberg EV. Cell-type-specific activation and repression of PU. 1 by a complex of discrete, functionally specialized cis-regulatory elements. *Mol Cell Biol.* 2010;30(20): 4922-4939.
44. Rosenbauer F, Tenen DG. Transcription factors in myeloid development: balancing differentiation with transformation. *Nat Rev Immunol.* 2007;7(2): 105-117.
45. Orkin SH. Diversification of haematopoietic stem cells to specific lineages. *Nat Rev Genet.* 2000; 1(1):57-64.
46. Yu C, Cantor AB, Yang H, et al. Targeted deletion of a high-affinity GATA-binding site in the GATA-1 promoter leads to selective loss of the eosinophil lineage in vivo. *J Exp Med.* 2002;195(11):1387-1395.
47. Hoogenkamp M, Lichtinger M, Krysinska H, et al. Early chromatin unfolding by RUNX1: a molecular explanation for differential requirements during specification versus maintenance of the hematopoietic gene expression program. *Blood.* 2009; 114(2):299-309.
48. Hoogenkamp M, Krysinska H, Ingram R, et al. The PU.1 locus is differentially regulated at the level of chromatin structure and noncoding transcription by alternate mechanisms at distinct developmental stages of hematopoiesis. *Mol Cell Biol.* 2007;27(21):7425-7438.
49. Laslo P, Spooner CJ, Warmflash A, et al. Multilineage transcriptional priming and determination of alternate hematopoietic cell fates. *Cell.* 2006; 126(4):755-766.
50. Lin YC, Jhunjhunwala S, Benner C, et al. A global network of transcription factors, involving E2A, EBF1 and Foxo1, that orchestrates B cell fate. *Nat Immunol.* 2010;11(7):635-643.
51. Walsh JC, DeKoter RP, Lee HJ, et al. Cooperative and antagonistic interplay between PU.1 and GATA-2 in the specification of myeloid cell fates. *Immunity.* 2002;17(5):665-676.